Identification of Multiple faults in an Inertial Measurement Unit

Cédric Berbra, Sylviane Gentil, Suzanne Lesecq

▶ **To cite this version:**

Cédric Berbra, Sylviane Gentil, Suzanne Lesecq. Identification of Multiple faults in an Inertial Measurement Unit. ACD 2009 - 7th European Workshop on Advanced Control and Diagnosis, Nov 2009, Zielona Gora, Poland. 6p. ⟨hal-00423555⟩

HAL Id: hal-00423555

https://hal.science/hal-00423555v1

Submitted on 12 Oct 2009

HAL is a multi-disciplinary open access archive for the deposit and dissemination of scientific research documents, whether they are published or not. The documents may come from teaching and research institutions in France or abroad, or from public or private research centers.

L'archive ouverte pluridisciplinaire **HAL**, est destinée au dépôt et à la diffusion de documents scientifiques de niveau recherche, publiés ou non, émanant des établissements d'enseignement et de recherche français ou étrangers, des laboratoires publics ou privés.

HAL Authorization

Identification of Multiple faults in an Inertial Measurement Unit

C. Berbra * **S. Gentil** * **S.Lesecq** **

* *Gipsa-lab, Control Systems Department, UMR-5216 BP.46, St Martin d'Heres, 38402, France(e-mail: author@gipsa-lab.grenoble-inp.fr).*
** *Commissariat a l'Energie Atomique (CEA-LETI MINATEC) 17, rue des Martyrs, 38054 Grenoble, France. e-mail: suzanne.lesecq@cea.fr*

Abstract: This paper deals with the diagnostic design of an Inertial Measurement Unit (IMU). IMU are widely used for system positioning. Their goal is to sense the attitude (or orientation) of a rigid body on which the IMU is embedded. In this paper, the sensors used in the IMU are a tri-axis accelerometer, a tri-axis magnetometer and 3 rate gyros. The diagnostic method proposed in this paper is independent of the physical system in which the IMU is embedded. This makes the diagnostic results very robust to disturbances or to imprecise knowledge of physical parameters. Moreover, the method proposed allows multiple faults isolation and identification. The simulation results are obtained with Matlab/Simulink.

Keywords: Fault diagnosis, fault detection, fault isolation, fault identification, multiple faults, optimization, Inertial Measurement Unit.

1. INTRODUCTION

This paper deals with the diagnostic design of an Inertial Measurement Unit (IMU). An IMU is an electronic device that measures and reports on a vehicle velocity, orientation, and gravitational forces, using a combination of accelerometers, magnetometers and rate-gyros. An IMU senses the current rate of acceleration using one or more accelerometers, and detects changes in rotational attributes such as pitch, roll and yaw angles using one or more rate-gyros and magnetometers. The data collected from the IMU sensors allows a computer to track a rigid body position and attitude (orientation). IMUs are typically used to maneuver aircrafts, including Unmanned Aerial Vehicles (UAVs), among many others, and spacecrafts, including shuttles, satellites and landers. Besides navigational purposes, low-cost IMUs are also used nowadays as orientation sensors in the field of human motion. They are for instance frequently used for sports technology, patient or senior monitoring, capture technology and animation. Nevertheless, they are not very robust and can present many kinds of faults. It is thus interesting to develop Fault Detection and Isolation (FDI) for IMUs together with Fault Tolerant Control (FTC) for systems that embed IMUs.

GIPSA-lab has developed a quadrotor as a test-bench for advanced control and diagnostic techniques. A quadrotor is an UAV with four rotors, each motor driving a blade. This quadrotor is equipped with an IMU. From its measurements, the attitude of the quadrotor is computed and then used in a state observer and a control loop (Guerrero-Castellanos et al. (2008), Guerrero-Castellanos et al. (2005)). UAV diagnosis has also been intensely studied during the last few years. For instance, FDI techniques have been applied to autonomous aircrafts (Simani et al. (2006))(Bonfe et al. (2009)), or to small autonomous helicopters (Heredia et al. (2008)). In (Henry (2008), Issury and Henry (2009), Patton et al. (2006)), FDI techniques are applied in aeronautics and aerospace areas. Our team has also proposed some solutions to the diagnostic problem of UAV (Tanwani et al. (2007), Berbra et al. (2008a)), being aware that the most important quadrotor component likely to fail is the IMU. FTC solutions have also been proposed (Berbra et al. (2008b)).

Diagnosis includes fault detection and isolation (FDI) but another important point is fault identification. Fault identification consists in estimating the fault amplitude and its temporal behavior, which is helpfull for the FTC of a system. In our previous works (Tanwani et al. (2007), Berbra et al. (2008a)), a bank of observers has been used to design structured residuals based on the quadrotor state estimation. The major difficulty in the solutions proposed in the latter papers is that the diagnostic algorithm is sensitive to the quadrotor model uncertainty or to disturbances on the quadrotor. Moreover, fault identification and multiple fault detection is not possible. These drawbacks constituted the motivation of the work presented in the present paper.

The simulation results have been obtained with Matlab/Simulink to simulate the quadrotor model, its control, observation and diagnosis. In order to postpone real experiments until everything has been carefully checked, an effcient way to simulate a system whose safety is critical is a hardware-in-the-loop approach. Such an experiment has been conducted for the quadrotor (Berbra et al. (2009)).

This paper is organized as follow: section 2 briefly presents the Inertial Measurement Unit model. Section 3 describes the diagnostic algorithm that has been developed for the IMU and that is completely independent of the experiment. The residual generation is fully described and some simulation results are discussed. Section 4 concludes this paper.

2. DESCRIPTION OF THE INERTIAL MEASUREMENT UNIT

2.1 Description of a rigid body orientation

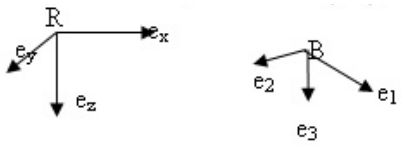

Fig. 1. Definition of the coordinate frames

To depict the orientation of a rigid body subject to movements, two frames are considered (see Fig. 1): the *inertial frame* $\mathbf{R}(e_x, e_y, e_z)$ and the *body frame* $\mathbf{B}(e_1, e_2, e_3)$. The inertial frame is attached to the earth and a classical choice is the NED frame (North, East, Down). The body frame is attached to the structure with its origin at the centre of mass of the body.

In the following paragraphs, the focus is done on orientation, also named attitude. Orientation can be expressed by three angles yaw-pitch-roll (ϕ, θ, ψ) or by a unitary quaternion $q \in \Re^4$ (Chou (1992))

$$q = [q_0 \quad \overrightarrow{q}^T]^T, \quad \|q\|_2 = 1 \tag{1}$$

The advantage of using q for the attitude representation is to avoid singularities that appear with classical angular representations (Euler angles or Cardan angles). Moreover, q is an elegant and efficient attitude representation from a computational point of view, which is of great importance for embedded systems. The quaternion representation is chosen in the present paper to perform computations. However, the simulation results will be presented in the roll-pitch-yaw formulation because it is more intuitive and thus easier to interpret the curves.

A coordinate change from $\overrightarrow{r}$ in the reference frame to $\overrightarrow{c}$ in the body frame is expressed with

$$c = q^{-1} \otimes r \otimes q = \overline{q} \otimes r \otimes q \tag{2}$$

where $r = [0 \ \overrightarrow{r}^T]^T$, $c = [0 \ \overrightarrow{c}^T]^T$. $\overline{q} = [q_0 \ -\overrightarrow{q}^T]$ is the conjugate of q and $\otimes$ is the quaternion multiplication.

Moreover, the coordinate change can be represented with matrix $C(q)$ that is expressed as

$$C(q) = (q_0^2 - \overrightarrow{q}^T\overrightarrow{q})I + 2(\overrightarrow{q}\,\overrightarrow{q}^T - q_0[q^\times]) \tag{3}$$

$$\overrightarrow{c} = C(q)\,\overrightarrow{r} \tag{4}$$

with

$$[q^\times] = \begin{pmatrix} 0 & -q_3 & q_2 \\ q_3 & 0 & -q_1 \\ -q_2 & q_1 & 0 \end{pmatrix} \tag{5}$$

2.2 Inertial Measurement Unit (IMU) modeling

The estimation of attitude (or orientation) and of rotational speed of a rigid body (the quadrotor for example) is a pre-requisite for its attitude control. An IMU can be embedded in the system in order to provide measurements that will be fused to estimate the attitude. The IMU consists of a tri-axis accelerometer (a_1, a_2, a_3), a tri-axis magnetometer (m_1, m_2, m_3) and three rate gyros (g_1, g_2, g_3) mounted at right angles.

Rate Gyro modeling The angular velocity ω is measured in the body frame $\mathbf{B}$ with the three rate gyros. The measurements delivered by these sensors are affected by noise. Theoretically, the integral of ω could give the relative orientation but the presence of noise generates errors that are accumulated over time. As a consequence, state observers are prefered. The sensor measurements are modeled as

$$\omega_g = \omega + \eta_{gyro} \tag{6}$$

where $\omega_g \in \Re^3$ are the sensor readings, $\omega \in \Re^3$ represents the system angular velocity and η_{gyro} is assumed to be a zero-mean white noise of appropriate dimension. Note that $\eta_{gyro} = 0.01\ rad/s$.

Accelerometer modeling The 3-axis accelerometer senses the inertial forces and gravity in $\mathbf{B}$. The transformation of accelerometer measurements from inertial frame $\mathbf{R}$ to body frame $\mathbf{B}$ is computed as follows

$$b_{acc} = C(q)(\dot{v} - g) + \eta_{acc} \tag{7}$$

where $b_{acc} \in \Re^3$ corresponds to the measurements in $\mathbf{B}$, and η_{acc} is a zero-mean white noise of appropriate dimension. The motion is supposed quasi-static so that linear accelerations $\dot{v}$ are neglected (i.e. $\|\dot{v}\| \ll \|g\|$). In this way, accelerometers are only sensitive to the gravitational field g. Note that measurements are normalized. Therefore $g = [0\ 0\ 1]^T$. Note that $\eta_{acc} = 0.002\ m/s^2$.

Magnetometer modeling The information provided by the tri-axis magnetometer is added to the inertial measurements. The magnetic field is sensed in $\mathbf{B}$. It is defined by

$$b_{mag} = C(q)h_m + \eta_{mag} \tag{8}$$

where $h_m = [h_{mx}\ 0\ h_{mz}]^T$ and $b_{mag} \in \Re^3$ are the magnetic field in $\mathbf{R}$ and $\mathbf{B}$, respectively. For the experimentation, $h_m = [\frac{1}{2}\ 0\ \frac{\sqrt{3}}{2}]^T$. Note that $\eta_{mag} = 0.0007\ mgauss$.

Remark Note that the accelerometer and magnetometer measurements are modeled by static non linear equations (7)-(8) that depend on constant vectors g and h_m and on matrix $C(q)$ which is a non-linear function of q.

2.3 Quadrotor control-loop

The diagnostic technique proposed in this paper is exemplified on a quadrotor that is under development at GIPSA-Lab. For this system, a non linear attitude observer has been designed (Guerrero-Castellanos et al. (2005)). The quaternion estimation q_{est} is used in a feedback loop. The attitude reference is given by a quaternion reference (see Fig. 2). The controller implemented for the

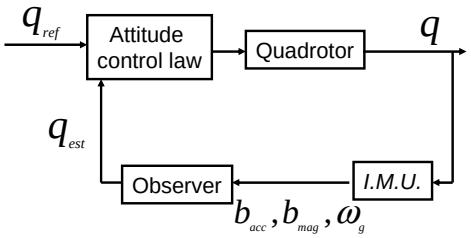

Fig. 2. Quadrotor control-loop

attitude stabilization is detailed in (Guerrero-Castellanos et al. (2008)). The quadrotor control loop performance can be evaluated with the following scenario. The initial attitude of the quadrotor is $[\phi\ \theta\ \psi] = [-25\ \ -35\ \ -10]^o$ where the unity is degrees. The reference attitude is $[0\ 0\ 0]^o$.

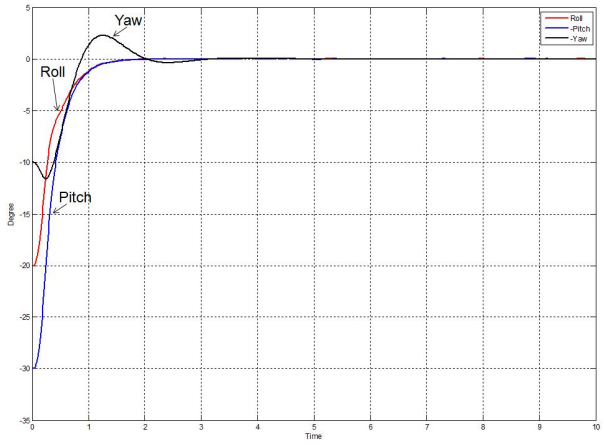

Fig. 3. Real attitude in the fault-free case

Fig. 3 shows the real attitude of the quadrotor in the fault-free case. The reference attitude is reached after 2.5 s.

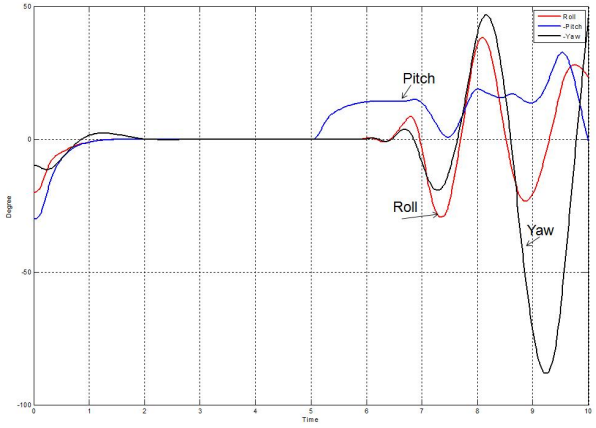

Fig. 4. Real attitude with a failure in a_1 at time $t = 5\ s$

Fig. 4 shows the real attitude of the quadrotor when a bias of 0.5 is introduced in a_1 at time $t = 5\ s$ (additive fault). When the sensor fault is not detected, the quadrotor crashes. Therefore, it is obvious that FDI must be implemented for safety issue.

3. DIAGNOSIS

To perform the diagnosis of the IMU, a bank of estimators/observators is implemented (Isermann (2006)),(Chen and Patton (1999)). Note that the technique proposed here is totally independent of the system in which the IMU is embedded. The residual generator is decomposed into two parts:

- Procedure 1: generation of the residuals that detect the accelerometer and magnetometer sensor faults. In this case, the rate gyro measurements are not used;
- Procedure 2: generation of the residuals that detect the rate-gyro sensor faults. In this case, the result obtained by the previous FDI algorithm for accelerometer and magnetometer faults is used to perform this diagnosis.

3.1 Procedure 1: accelerometers and magnetometers

Fig. 5 shows the structure of the procedure implemented here. The accelerometer and magnetometer measurements satisfy the set of six non-linear equations (7)-(8). The residuals are generated as follow:

(1) the attitude $\hat{q}_i$, $i = 1:6$, is estimated from 5 over 6 measurements, where i corresponds to the measurement discarded (see Fig. 5). Therefore, $\hat{q}_i$ is the solution of a non linear optimization problem with constraint $\|q\| = 1$ (Berbra et al. (2008a)) or (Tanwani et al. (2007));
(2) with $\hat{q}_i$, the measurements are estimated with the measurement model (7)-(8);
(3) the residual vector $R_i \in \Re^6$ is computed in a classical way (difference between measurements and their estimates).

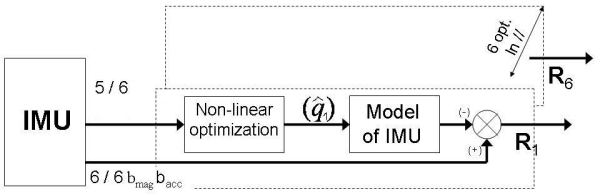

Fig. 5. Residuals generation for accelerometer and magnetometer sensors

Note that R_i is sensitive to faults in all the sensors used to compute $\hat{q}_i$. Thus R_i is insensitive to faults in sensor i. The fault signature table is given in Table 1.

Table 1. Fault signature table to isolate accelerometer and magnetometer sensor faults

	f_{a_1}	f_{a_2}	f_{a_3}	f_{m_1}	f_{m_2}	f_{m_3}
R_1	[10..0]	[1..1]	[1..1]	[1..1]	[1..1]	[1..1]
R_2	[1..1]	[010..0]	[1..1]	[1..1]	[1..1]	[1..1]
R_3	[1..1]	[1..1]	[001000]	[1..1]	[1..1]	[1..1]
R_4	[1..1]	[1..1]	[1..1]	[000100]	[1..1]	[1..1]
R_5	[1..1]	[1..1]	[1..1]	[1..1]	[0..010]	[1..1]
R_6	[1..1]	[1..1]	[1..1]	[1..1]	[1..1]	[0..01]

$R_i, i = 1:6$, is the set of vectorial residuals obtained when $\hat{q}_i$ is estimated without $a_1, a_2, a_3, m_1, m_2, m_3$ respectively. The columns of Table 1 represent the faults in the six sensors. [111111] means that the residual elements are

computed with a faulty sensor (i.e. the faulty sensor is in the set of sensors used to estimate $\hat{q}_i$). [100000] corresponds to residual elements computed without the faulty sensor. Therefore, the faulty sensor can be isolated.

Consider a fault in a_1 identical to the one in section (2.3). For the sake of place, only two over six residual vectors are presented. Fig. 6 shows R_1 computed without sensor a_1. As expected, only the first element in R_1 is sensitive to the fault (see the first column in Table 1). Note that the magnitude of the first component in R_1 is equal to the magnitude of the fault introduced. Therefore, the sensor fault is detected, isolated and *identified*. Fig. 7 depicts R_6 computed without m_3. All the components of R_6 are sensitive to the fault because a_1 is taken into account for the estimation of $\hat{q}_6$.

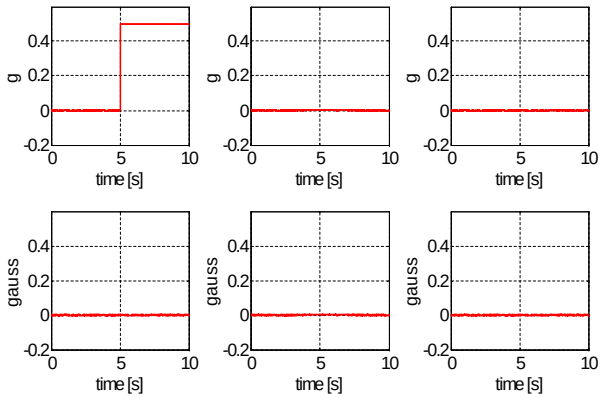

Fig. 6. Residual vector R_1 in presence of a fault in a_1 at time $t = 5\ s$

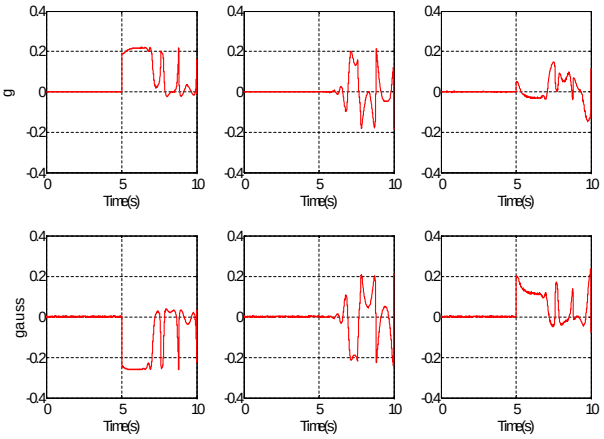

Fig. 7. Residual vector R_6 in presence of a fault in a_1 at time $t = 5\ s$

3.2 Procedure 2: FDI for rate gyros

The rate-gyro measurements satisfy the dynamic non-linear equation

$$\dot{q} = \begin{pmatrix} \dot{q}_0 \\ \dot{\overrightarrow{q}} \end{pmatrix} = \frac{1}{2} \begin{pmatrix} -\overrightarrow{q}^{\,T} \\ I_3 q_0 + [\overrightarrow{q}^{\times}] \end{pmatrix} \omega \qquad (9)$$

Eq. (9) is approximated to provide the diagnosis of rate gyros. The diagnostic procedure implemented is depicted in Fig. 8. It is summarized hereafter:

(1) the FDI algorithm proposed in section (3.1) to obtain an unfaulty estimate of the attitude (i.e. the quaternion $\hat{q}_i$ computed without faulty sensor) is first used. Denote $\hat{q}(k)$ this attitude computed at time kT_e;
(2) $\hat{q}(k)$ is filtered to reduce the noise. The filter is designed as follows:

$$H(z) = \frac{(1-\alpha)z^{-1}}{1-\alpha z^{-1}} \qquad (10)$$

with $\alpha = e^{\frac{-T_e}{\tau}}$, and $T_e = 10\ ms$ the sampling period;
(3) the filtered attitude is derived to obtain $\dot{\hat{q}}$. This derivative is obtained with the following approximation:

$$\frac{d\hat{q}}{dt} \approx \frac{\hat{q}_{filter}(k) - \hat{q}_{filter}(k-1)}{T_e} \qquad (11)$$

(4) With $\hat{q}$ and $\dot{\hat{q}}$, solve (9) in a least squares sense to compute $\hat{\omega}_i$;
(5) the residual vector $r_{\omega i}$, $i = 1:3$, is the difference between the measurements and their estimates.

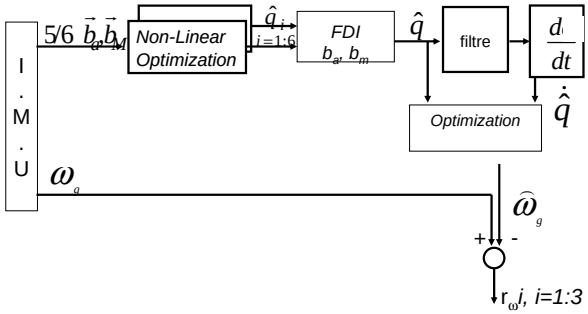

Fig. 8. Residual generation for rate gyros

Note that this procedure allows simultaneous rate gyro sensor faults detection, isolation and identification. The associated fault signature table is given in table 2.

Table 2. Fault signature table to isolate rate-gyro sensor faults

	f_{g_1}	f_{g_2}	f_{g_3}
r_{ω_1}	1	0	0
r_{ω_2}	0	1	0
r_{ω_3}	0	0	1

As an example, consider a bias failure of $0.1\ rad/s = 5.7\ ^o/s$ on the rate gyro g_3 that appears at $t = 5\ s$. Fig. 9 shows the real attitude of the quadrotor if this sensor fault is not detected. It is clear that for safety reason, the rate gyro sensor faults must be diagnosed.

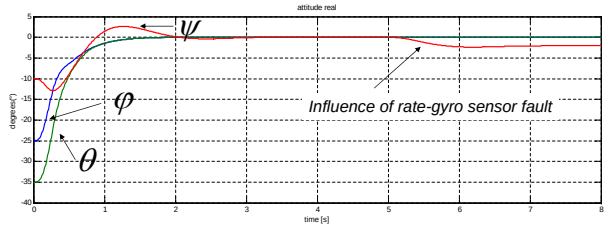

Fig. 9. Real attitude of the quadrotor with a fault in g_3 at time $t = 5\ s$

Fig. 10 shows the residual vector r_ω expressed in rad/s . As expected, only the residual $r_{\omega 3}$ is sensitive to this sensor fault.

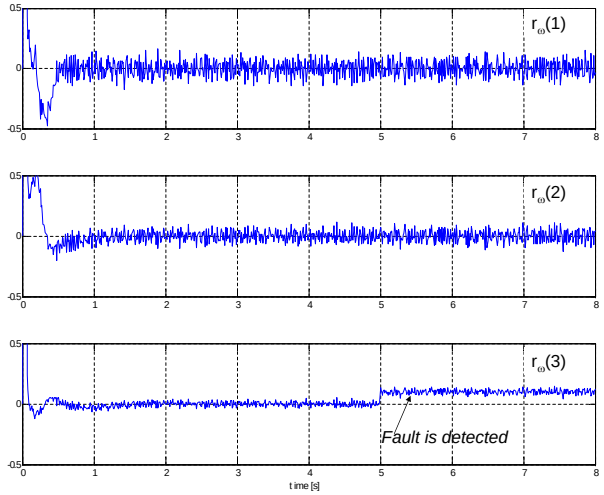

Fig. 10. Residual vector to detect rate-gyro sensor faults

Consider the following scenario: the reference attitude is first equal to $[\phi\ \theta\ \psi] = [0\ 0\ 0]^o$. At time $t = 5\ s$, the reference attitude becomes $[\phi\ \theta\ \psi] = [10\ -20\ 5]^o$. Fig. 11 shows the real attitude of the quadrotor in the fault-free case. The first reference attitude is reached after 2.5 s and the new attitude is attained after 1.5 s. Now consider that at the time the reference changes, two rate gyro sensor faults appear simultaneously: a bias failure of 0.5 rad/s is added on g_3 and a drift failure of 0.5 rad/s appears on g_1.

Fig. 12 shows the real attitude if these faults are not detected. The ϕ angle is very different from its nominal value and the system will crash.

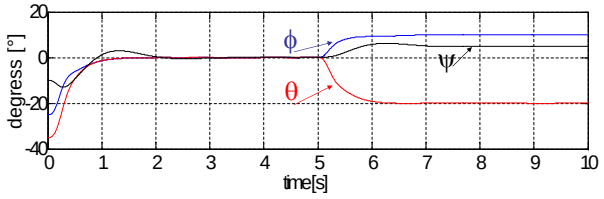

Fig. 11. Real attitude in the fault-free case

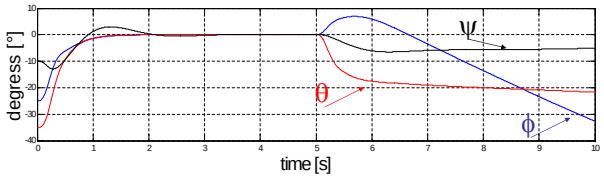

Fig. 12. Real attitude with simultaneous faults in g_1 and g_3

Fig. 13 shows the residual vector r_ω. As can be seen, $r_{\omega 1}$ is sensitive only to the drift failure in g_1 and its magnitude is equal to the magnitude of the fault. In the same way, $r_{\omega 3}$ is sensitive only to the bias failure in g_3 and its magnitude is equal to the magnitude of the failure. $r_{\omega 2}$ is insensitive to both failures. Moreover, all residuals are insensitive to a reference change.

3.3 FDI results in the presence of a disturbance

A complex problem tackled by the diagnostic community is developing residual generators insensitive to model

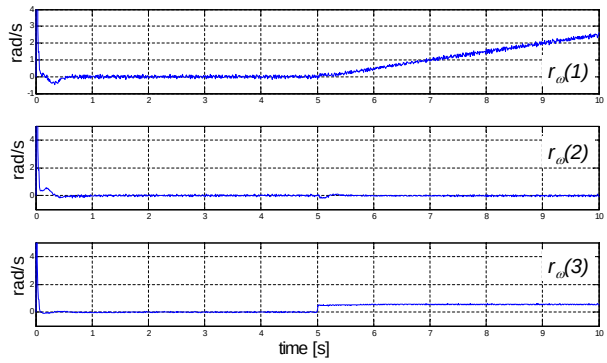

Fig. 13. Residual vector to detect simultaneous rate-gyro sensors faults

uncertainty and real disturbances acting on the system to diagnose while remaining sensitive to faults. A step disturbance of 2^o in applied on each angle. The objective is to evaluate the robustness of the residual generator proposed in the present paper against disturbances. Theses disturbances could represent a gust of wind.

Fig. 14 shows the residual vector R_1 in the presence of the disturbances. Remind that R_1 is computed without a_1. Fig. 15 shows the residual vector r_ω. As can be seen, the proposed FDI algorithm is totally insensitive to these disturbances because it does not rely on the dynamic model of the rigid body on which the IMU is fixed.

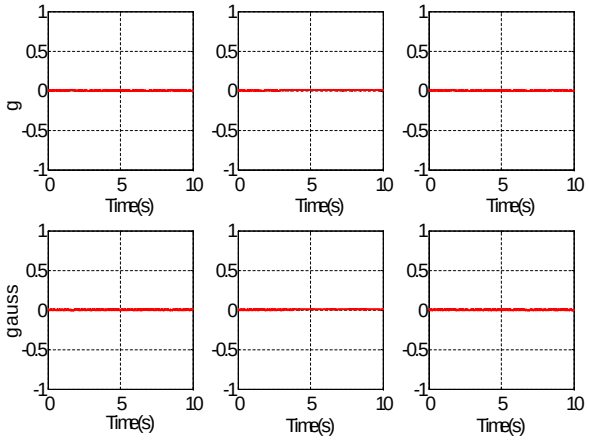

Fig. 14. R_1 in the presence of a disturbance

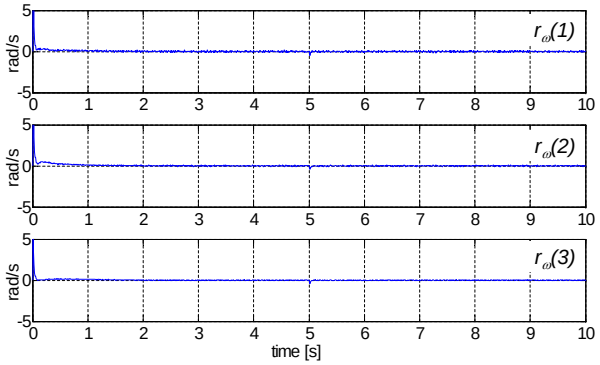

Fig. 15. Residual vector r_ω in presence of a disturbance

4. CONCLUSION AND PERSPECTIVES

A new method to perform FDI of an Inertial Measurement Unit is proposed in this paper. A bank of estimators has been implemented that take advantage of information redundancy. Actually there is no sensor redundancy, but the various sensors sense complementary and redundant information. From the attitude estimate and the measurement models, the residuals can be computed as the difference between the measurements and their estimates. A strongly isolating table is obtained. Contrary to (Berbra et al. (2008a)) or (Tanwani et al. (2007)), the method proposed in the present paper is insensitive to a disturbance applied on the rigid body in which the IMU is embedded. Moreover, it is insensitive to an uncertainty in the dynamic model of the rigid body, for instance an uncertainty in the inertia matrix of the rigid body. This nice property exists because the model of the rigid body is no more used for diagnosis. Additionally, with the method proposed, the fault identification can be performed and simultaneous sensors faults can be considered. It is important to note that the FDI procedures proposed here are general ones and can be applied to any system that makes use an Inertial Measurement Unit to estimate attitude.

This new algorithm must now be tested for the quadrotor application. Note that a first step will be to use an "hardware in the loop" experiment (Berbra et al. (2009)) because the system embeds a network on which the data from the IMU as transmitted to the processor unit.

For the quadrotor application, a Fault Tolerant Control could be implemented to take into account the sensor faults. As the magnitude of the residuals are the same as the magnitude of the faults, the FTC can be expected to be easier. Moreover, when faulty sensors are isolated, only the unfaulty measurements could be used by the state observer. Due to redundancy in the information sensed by the sensors, this observer can be exploited with partial measurement loss (Lesecq et al., 2009). Thus the control law would not need to be modified.

ACKNOWLEDGEMENTS

This work is partially supported by the Safe-NeCS project funded by the Agence Nationale de la Recherche (France) under grant ANR-05-SSIA-0015-03

REFERENCES

Berbra, C., Gentil, S., Lesecq, S., and Thiriet, J.M. (2008a). Co-design of a safe network control quadrotor. In *17th IFAC World Congress*. Seoul,Korea.

Berbra, C., Lesecq, S., and Martinez, J.J. (2008b). A Multi-Observer Switching Strategy for Fault-Tolerant Control of a Quadrotor Helicopter. In *16th Mediterranean Conference on Control and Automation, IEEE-MED08*. Ajaccio, France.

Berbra, C., Simon, S., Gentil, S., and Lesecq, S. (2009). Hardware in the loop networked control and diagnosis of a quadrotor drone. In *7th IFAC Symposium on Fault Detection, Supervision and Safety of Technical Processes, SafeProcess*. Barcelona, Spain.

Bonfe, M., Simani, S., and Castaldi, P. (2009). Active Fault Tolerant Control Scheme for a General Aviation Aircraft Model. In *17th Mediterranean Conference on Control and Automation, IEEE-MED09*. Thessaloniki, Greece.

Chen, J. and Patton, R. (1999). *Robust Model-Based Fault Diagnosis for Dynamic Systems*. Kluwer Academic Publishers.

Chou, J.C. (1992). Quaternion kinematic and dynamic differential equations. *IEEE Transactions on Robotics and Automation*, 8, 53–64.

Guerrero-Castellanos, J., Lesecq, S., Marchand, N., and Delamare, J. (2005). A low-cost air data attitude heading reference system for the tourism airplane applications. In *IEEE Conference Sensors 2005*.

Guerrero-Castellanos, J., Marchand, N., Lesecq, S., and Delamare, J. (2008). Bounded attitude stabilization: Real-Time application on four-rotor helicopter. In *17th IFAC World Congress*. Seoul, Korea.

Henry, D. (2008). From fault diagnosis to recovery actions for aeronautic and aerospace missions: a model-based point of view. In *23rd IAR Workshop on Advanced Control and Diagnosis, IAR-ACD*. Coventry, UK.

Heredia, G., Oilero, A., Bejar, M., and Mahtani, R. (2008). Sensor and actuator fault detection in small autonomous helicopter. *Mechatronics*, 18, 90–99.

Isermann, R. (2006). *Fault-Diagnosis Systems: An Introduction from Fault Detection to Fault Tolerance*. Springer.

Issury, I. and Henry, D. (2009). Multiple and simultaneous fault isolation with minimal fault indicating signals: a case study. In *7th IFAC Symposium on Fault Detection, Supervision and Safety of Technical Processes, SafeProcess*. Barcelona, Spain.

Lesecq, S., Gentil, S., and Daraoui, N. (2009). Quadrotor attitude estimation with data losses. In *European Control Conference ECC09*. Budapest, Hungary.

Patton, R., Uppal, F., Simani, S., and Polle, B. (2006). A Monte Carlo analysis and design for FDI of a satellite control system. In *6th IFAC Symposium on Fault Detection, Supervision and Safety of Technical Processes, SafeProcess*. Beijing, China.

Simani, S., Bonfe, M., and Geri, W. (2006). Application of Fault Diagnosis methodologies to a general aviation aircraft. In *6th IFAC Symposium on Fault Detection, Supervision and Safety of Technical Processes, SafeProcess*. Beijing, China.

Tanwani, A., Lesecq, S., Gentil, S., and Thiriet, J. (2007). Experimental networked embedded minidrone- part II. Distributed FDI. In *European Control Conference ECC07*. Kos, Greece.